

Lewis X-carrying *N*-Glycans Regulate the Proliferation of Mouse Embryonic Neural Stem Cells via the Notch Signaling Pathway^{*S}

Received for publication, March 23, 2012, and in revised form, May 10, 2012. Published, JBC Papers in Press, May 29, 2012, DOI 10.1074/jbc.M112.365643

Hirokazu Yagi^{‡1}, Takuya Saito[‡], Makoto Yanagisawa[§], Robert K. Yu^{§2}, and Koichi Kato^{‡¶3}

From the [‡]Graduate School of Pharmaceutical Sciences, Nagoya City University, 3-1 Tanabe-dori, Mizuho-ku, Nagoya 467-8603, Japan, the [§]Institute of Molecular Medicine and Genetics and Institute of Neuroscience, Medical College of Georgia, Georgia Health Sciences University, Augusta, Georgia 30912, and the [¶]Institute for Molecular Science and Okazaki Institute for Integrative Bioscience, National Institutes of Natural Sciences, 5-1 Higashiyama Myodaiji, Okazaki 444-8787, Japan

Background: Glycosylation is known to be altered upon differentiation of neural stem cells (NSCs).

Results: NSC-specific Lewis X-carrying *N*-glycans up-regulated the expression of Musashi-1 and the consequent cell proliferation.

Conclusion: Lewis X operates as an activator of the Notch signaling pathway for the maintenance of NSC stemness.

Significance: The well known undifferentiation glycomarker of NSCs is actively involved in their fate determination.

Neural stem cells (NSCs) possess high proliferative potential and the capacity for self-renewal with retention of multipotency to differentiate into brain-forming cells. Several signaling pathways have been shown to be involved in the fate determination process of NSCs, but the molecular mechanisms underlying the maintenance of neural cell stemness remain largely unknown. Our previous study showed that human natural killer carbohydrate epitopes expressed specifically by mouse NSCs modulate the Ras-MAPK pathway, raising the possibility of regulatory roles of glycoprotein glycans in the specific signaling pathways involved in NSC fate determination. To address this issue, we performed comparative *N*-glycosylation profiling of NSCs before and after differentiation in a comprehensive and quantitative manner. We found that Lewis X-carrying *N*-glycans were specifically displayed on undifferentiated cells, whereas paucimannose-type *N*-glycans were predominantly expressed on differentiated cells. Furthermore, by knocking down a fucosyltransferase 9 with short interfering RNA, we demonstrated that the Lewis X-carrying *N*-glycans were actively involved in the proliferation of NSCs via modulation of the expression level of Musashi-1, which is an activator of the Notch signaling pathway. Our findings suggest that Lewis X carbohydrates, which have so far been characterized as undifferentiation markers, actually operate as activators of the Notch signaling

pathway for the maintenance of NSC stemness during brain development.

Neural stem cells (NSCs)⁴ are undifferentiated neural cells that are characterized by a high proliferative potential and the capacity for self-renewal with retention of multipotency to differentiate into neurons, astrocytes, and oligodendrocytes (1–3). In postnatal and adult mammalian brains, NSCs are localized in the subventricular zone of the lateral ventricles and the subgranular layer of the dentate gyrus in the hippocampus (4–6). To identify NSCs in these regions, several markers such as Nestin, Sox2, CD133, Musashi-1, and the stage-specific embryonic antigen-1 (SSEA-1/Lewis X/CD15) have been utilized (7–12). Musashi-1, one of these NSC markers, plays a crucial role in maintaining the undifferentiated state of NSCs via activation of the Notch signaling pathway (13, 14). In addition, the Wnt, Ras-MAPK, and JAK/STAT signaling pathways regulate the process for determining the fate of NSCs (self-renewal, proliferation, differentiation, survival, and death) through the interaction between specific cell surface receptors and environmental factors, such as growth factors, extracellular matrix, and cell adhesion molecules (15–19). Understanding the molecular mechanisms underlying NSC fate determination is of vital importance for the application of NSCs in cell replacement therapy for neurological diseases. The transplantation of NSCs can have therapeutic effects in animals with central nervous system damage (20, 21), but it is currently difficult to fully control the maintenance and differentiation of NSCs. This shows that the signaling mechanisms that regulate NSC fate remain largely unknown.

* This work was supported, in whole or in part, by National Institutes of Health Grant NS11853 (to R. Y.) from USPHS. This work was also supported by the Naito Foundation and Grants-in-aid for Young Scientists (B) 22790076 (to H. Y.) and Scientific Research on Innovative Areas (No. 23110002, Deciphering sugar chain-based signals regulating integrative neuronal functions) (to H. Y.) from the Ministry of Education, Culture, Sports, Science and Technology of Japan.

^S This article contains supplemental Figs. 1–4 and Tables 1 and 2.

¹ Supported by the Japan-United States Brain Research Cooperative Program.

² To whom correspondence may be addressed: Institute of Molecular Medicine and Genetics and Institute of Neuroscience, Medical College of Georgia, Georgia Health Sciences University, Augusta, GA 30912. Tel.: 706-721-0699; Fax: 706-721-8727; E-mail: rkyu@georgiahealth.edu.

³ To whom correspondence may be addressed: Institute for Molecular Science and Okazaki Institute for Integrative Bioscience, National Institutes of Natural Sciences, 5-1 Higashiyama Myodaiji, Okazaki 444-8787, Japan. Tel.: 81-564-59-5225; Fax: 81-564-59-5224; E-mail: kkatonmr@ims.ac.jp.

⁴ The abbreviations used are: NSC, neural stem cell; FUT9, fucosyltransferase 9; HNK-1, human natural killer-1; LAMP-1, lysosomal-associated membrane protein 1; ODS, octadecylsilica; Pax6, paired box protein 6; SSEA-1, stage-specific embryonic antigen-1; SOX2, sex-determining region Y-box 2; TNC, tenascin-C; WST-8, 2-(2-methoxy-4-nitrophenyl)-3-(4-nitrophenyl)-5-(2,4-disulfophenyl)-2H-tetrazolium; PA, pyridylaminated.

Recently, we showed that mouse NSCs specifically express the extracellular matrix protein tenascin-C (TNC), which is modified with human natural killer (HNK)-1 carbohydrate, and this glycoconjugate regulates cellular proliferation via modulation of the Ras-MAPK pathway (22). This study suggested that glycoprotein glycans might be active regulators that maintain the stemness of NSCs through specific signaling pathways, which prompted us to undertake comprehensive, quantitative glycosylation profiling of NSCs before and after differentiation. We report the comparative *N*-glycosylation profiles during the development of NSCs, wherein we found that Lewis X-carrying *N*-glycans were specifically expressed on glycoproteins produced by undifferentiated NSCs. We also reveal that these *N*-glycans were critically involved in regulating the proliferation of NSCs.

EXPERIMENTAL PROCEDURES

Antibodies—AK97 mouse monoclonal antibody (IgM), prepared from culture supernatants of an AK97 hybridoma cell line, was used as an anti-Lewis X antibody (23). Other antibodies used in this study are listed in supplemental Table 1.

NSC Culture—NSCs were prepared in the form of neurospheres according to methods described previously (22, 24). In brief, single cell suspensions prepared from the striata of ICR mouse embryos (embryonic day 14.5) were cultured in Neurobasal-A medium (Invitrogen) containing B27 serum-free supplement (Invitrogen), L-glutamine (Invitrogen), 20 ng/ml basic FGF (PeproTech, Rocky Hill, NJ), and 20 ng/ml of epidermal growth factor (EGF; PeproTech). Neurospheres formed after 5–6 days were collected for passage or analysis. To induce differentiation, the NSCs were cultured for 10 days in Neurobasal-A medium containing B27, L-glutamine (Invitrogen), and 1% fetal bovine serum in the absence of basic FGF and EGF.

***N*-Glycosylation Profiling**—All experimental procedures used for profiling, including the delipidation of cells, chromatographic conditions, glycosidase treatments, and matrix-assisted laser desorption/ionization time-of-flight mass spectrometry (MALDI-TOF-MS) and MS/MS techniques, have been described previously (25–29). In brief, *N*-glycans were released from delipidated cell lysates (1×10^7 cells) by hydrazinolysis and then labeled with 2-aminopyridine. PA-glycans were detected by fluorescence using excitation and emission wavelengths of 320 and 400 nm, respectively. The PA-glycan mixture was first separated on a TSKgel DEAE-5PW column (7.5-mm inner diameter \times 75 mm; Tosoh, Tokyo, Japan) at 30 °C with a flow rate of 1.0 ml/min using two solvents, A and B. Solvent A was aqueous ammonia (pH 9.0), and solvent B was a 50 mM ammonium acetate solution (pH 9.0). The column was equilibrated with solvent A. The gradient elution parameters were as follows: 0–3 min, linear gradient 0–12% B; 3–17 min, linear gradient 12–40% B; 17–22 min, linear gradient 40–100% B. Each oligosaccharide was separated according to its anionic charges. Each fraction separated from the DEAE column was collected, evaporated, and then applied to a Shim-pack HRC-octadecyl silica (ODS) column (6.0-mm inner diameter \times 150 mm; Shimadzu, Kyoto, Japan). Elution was performed at a flow rate of 1.0 ml/min at 55 °C using two solvents, C and D. Solvent C was 10 mM sodium phosphate buffer (pH 3.8), and solvent D

was 10 mM sodium phosphate buffer (pH 3.8) containing 0.5% 1-butanol. The gradient elution parameters were 0–60 min and a linear gradient of 20–50% solvent D. The fractions separated on the ODS column were subjected to MALDI-TOF-MS analysis, and the fractions possibly including two or more *N*-glycans were further separated using an amide column. Identification of *N*-glycan structures was based on their elution positions on the column, and their molecular mass values were compared with those of PA-glycans in the GALAXY database (26). The structures of PA-glycans that had not been registered in this HPLC database were characterized by exoglycosidase treatments and mass spectrometric techniques (30, 31).

Immunocytochemistry—NSCs prepared from neurospheres were plated onto chamber slides (Nalge Nunc International, Naperville, IL) coated with poly-L-ornithine (Sigma) and fibronectin (Sigma) and fixed in PBS containing 4% paraformaldehyde. The NSCs were treated for 2 h with PBS containing 3% fetal bovine serum and 0.1% Triton X-100 and then stained with primary antibodies such as Rat401 anti-nestin monoclonal antibody (BD Biosciences), AK97 anti-Lewis X monoclonal antibody (IgM), and anti- β -III tubulin monoclonal antibody (Sigma), and secondary antibodies as follows: anti-rat IgG antibody conjugated with Alexa Fluor 488 (BD Biosciences), anti-mouse IgM antibody conjugated with Alexa Fluor 595 (BD Biosciences), and anti-mouse IgG antibody conjugated with Alexa Fluor 488 (BD Biosciences). Nuclei were stained with 2 μ g/ml of Hoechst 33258 (Sigma).

Western Blot Analysis—NSCs and cells differentiated from NSCs were lysed in 500 μ l of lysis buffer (20 mM Tris-HCl (pH 7.6), 150 mM NaCl, 1 mM EDTA, and 1% Triton X-100) using a 1-ml syringe with a 26-gauge needle. The lysates were centrifuged for 10 min at $11,250 \times g$ at 4 °C. The resulting supernatant was used for protein analysis. Proteins in this fraction were subjected to 3–10% gradient SDS-PAGE and subsequently transferred to a polyvinylidene difluoride membrane (Bio-Rad). After blocking with Blocking One (Nacalai Tesque), the membrane was incubated with primary antibodies and then with horseradish peroxidase-conjugated secondary antibodies (supplemental Table 1). The protein bands were visualized using Western Lightning Chemiluminescence Reagent (PerkinElmer Life Sciences). To remove *N*-glycans on the glycoproteins, a lysate containing 20 μ g of proteins was incubated with peptide: *N*-glycosidase F (50 units; New England Biolabs, Beverly, MA) for 3 h at 37 °C before being subjected to SDS-PAGE.

Identification of Glycoproteins by LC/MS/MS Analysis—For liquid chromatography (LC)-MS/MS analysis to identify Lewis X-carrying protein, digestion of the glycoprotein was performed as described previously (22, 28).

RNA Interference—Negative control double-stranded RNAi was purchased from Qiagen (Valencia, CA). Small interfering RNAs (siRNAs) (19-mer) targeting FUT9 and LAMP-1 were purchased from Nippon EGT (Toyama, Japan). The corresponding target mRNA sequences for the siRNAs were as follows: GCAAGAGUAUUGAAAUCCA for FUT9 and UCACCUACCUGAAAAAGGA for LAMP-1. NSCs were transfected with siRNA using Lipofectamine RNAiMAX (Invitrogen) according to the manufacturer's instructions. In brief, NSCs cultured as neurospheres were triturated into single cells and

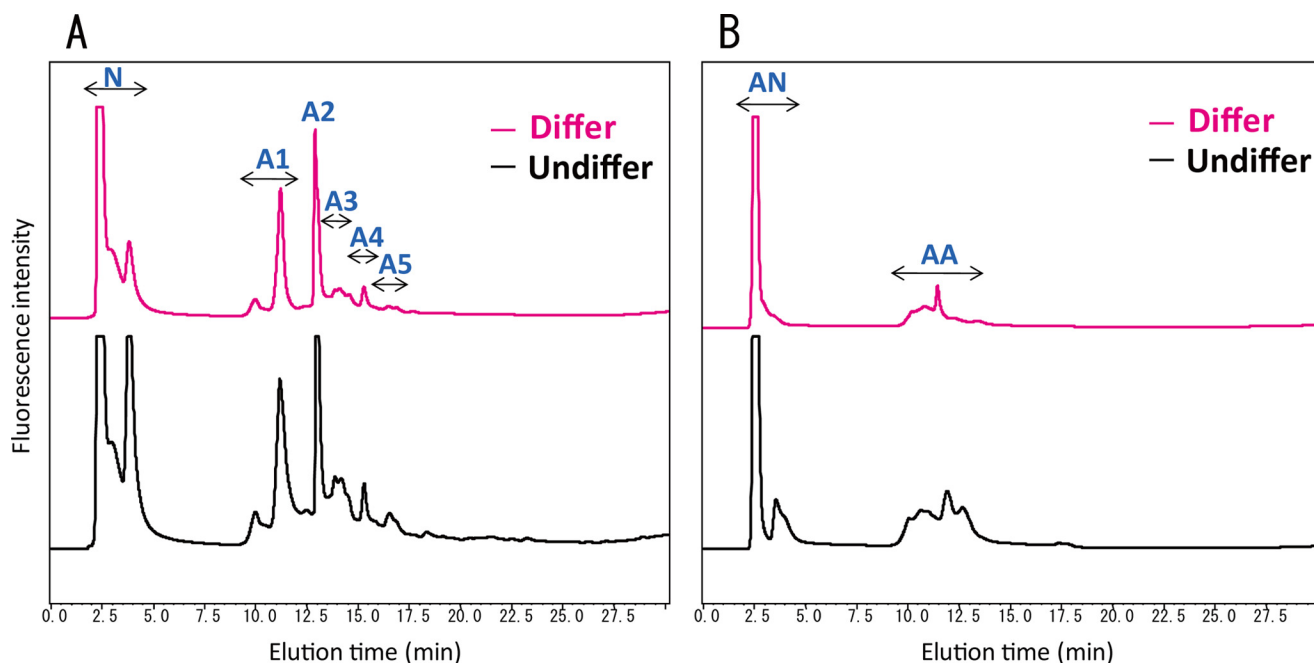


FIGURE 1. *N*-Glycosylation profiles on the DEAE column derived from NSCs before and after differentiation. *A*, PA-glycan mixtures were subjected to the DEAE column. The *N* and *A1–A5* fractions denote the neutral and anionic fractions, respectively. *A1–A5* denote the fractions of PA-*N*-glycans with 1–5 negative charges, respectively. *B*, mixture of anionic fractions *A1–A5* was digested by α -sialidase and then applied onto the DEAE column. *AN* and *AA* fractions denote the resultant neutral and anionic fractions, respectively. *Undiffer* and *Differ* indicate NSCs before and after differentiation, respectively.

transfected onto a 6-well plate using a reverse transfection method. The specific siRNA oligomers (24 pmol) were diluted in 400 μ l of Dulbecco's modified Eagle's medium and mixed with 4 μ l of Lipofectamine RNAiMAX. After a 20-min incubation at room temperature, the siRNA complexes were added to 4×10^5 NSCs. The NSCs transfected with the negative control siRNA were used as control. The RNAi results were evaluated by Western blotting with anti-HNK-1 or anti-TNC antibodies.

WST-8 Assay—NSC proliferation was assessed by a WST-8 assay using a Cell Counting Kit-8 (Dojindo, Kumamoto, Japan) (32, 33). In brief, siRNA-treated cells were transferred onto 96-well plates at a density of 2×10^5 cells/ml (100 μ l/well). After 24, 48, and 72 h of siRNA treatment, the cells were incubated for 4 h with WST-8, 2-(2-methoxy-4-nitrophenyl)-3-(4-nitrophenyl)-5-(2,4-disulfophenyl)-2*H*-tetrazolium, solution at 37 °C. The spectrophotometric absorbance of the WST-8-formazan produced by the dehydrogenase activity in the living cells was measured at a wavelength of 450 nm (reference, 650 nm), using a microplate spectrophotometer.

Quantitative Reverse Transcription (RT)-PCR Analysis—Quantitative RT-PCR was performed as described previously (22, 34). In brief, total RNAs were isolated from NSCs using TRIzol reagent (Invitrogen). cDNAs were synthesized from the total RNAs as templates using SuperScriptIII reverse transcriptase (Invitrogen). Quantitative PCR assays were run on ABI7300 (Applied Biosystems) using the following settings: 95 °C for 10 min, 1–40 cycles of 95 °C for 15 s, 55 °C for 15 s, 60 °C for 45 s, and 72 °C for 5 min; SYBR Green (Applied Biosystems) was used for detection. Primer sets used for PCR analysis are shown in supplemental Table 2. β -Actin was used as a control housekeeping gene.

Terminal Deoxynucleotidyltransferase-mediated dUTP Nick End-labeling (TUNEL) Assay—Apoptotic NSCs were detected with the TUNEL assay as described previously (22). The siRNA-transfected NSCs were plated onto chamber slides and cultured for 3 days. NSCs were then fixed for 1 h in PBS at room temperature containing 4% paraformaldehyde and permeabilized in 0.1% sodium citrate containing 0.1% Triton X-100 for 2 min at 4 °C. The cells were then stained with fluorescein-conjugated TUNEL reaction mixture (Roche Applied Science) for 2 h at 37 °C and then with Hoechst 33258 for 30 min.

RESULTS

***N*-Glycosylation Profile Alteration of Neural Stem Cells during Differentiation**—NSCs were isolated from the striata of mouse embryos (embryonic day 14.5) in the form of neurospheres, floating clonal aggregates formed by NSCs *in vitro* (24, 35). It has been shown that the cells forming neurospheres have self-renewal ability, express neural stem cell markers, and are capable of differentiating into neurons, astrocytes, and oligodendrocytes (22, 24).

The *N*-glycans from delipidated NSCs before and after differentiation were released by hydrazinolysis, labeled with 2-aminopyridine, and subsequently subjected to three-dimensional-HPLC profiling. Fig. 1*A* compares the *N*-glycosylation profiles on a DEAE anion-exchange column of the PA-glycans, separated into neutral and anionic fractions (*A1–A5*). Based on the fluorescence intensities of the individual fractions, the molar ratio of each fraction is shown in supplemental Fig. 1. The anionic fractions *A1–A5* were treated with sialidase to facilitate the identification of each of the anionic glycan fractions and then were subjected to the DEAE column for detection of the neo-neutral and still anionic fractions (Fig. 1*B*).

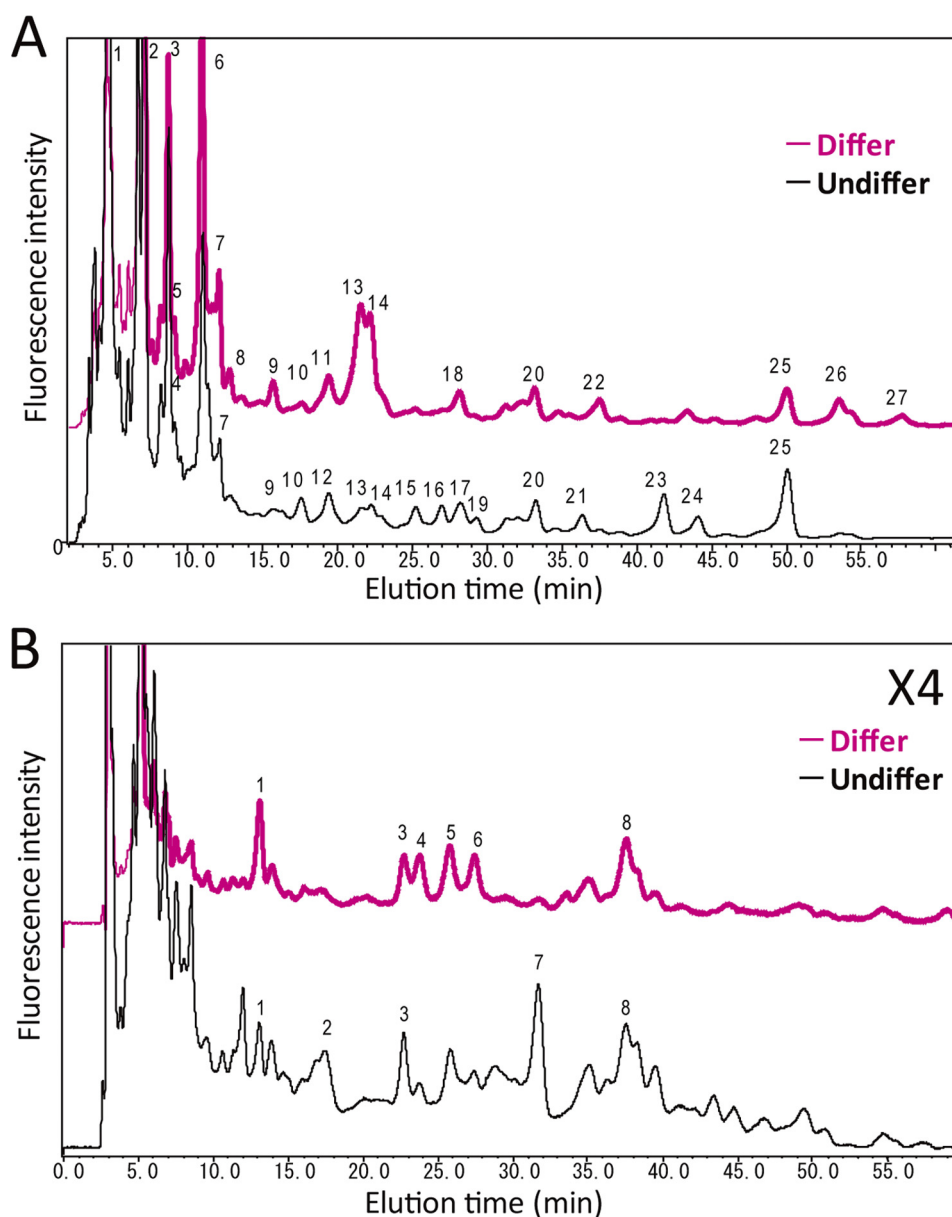


FIGURE 2. **N-Glycosylation profiles on the ODS column derived from NSCs before and after differentiation.** The fractions neo-neutral and still anionic separated by the DEAE column were individually applied onto the ODS column and they yielded elution profiles A and B, respectively. A and B, peaks were numbered in order of elution time. *Undiffer* and *Differ* indicate NSCs before and after differentiation, respectively.

Approximately 90% of total *N*-glycans were neutral oligosaccharides in both NSCs and the cells differentiated therefrom. The fractions neutral and neo-neutral were further applied to an ODS column (Fig. 2, A and B, respectively). Subsequently, the individual fractions separated from the ODS column were subjected to analysis by MALDI-TOF-MS. The *N*-glycan structures were identified based on their elution times and molecular mass values using the GALAXY database in conjunction with MALDI-TOF-MS/MS analysis and specific exoglycosidase digestion. Tables 1 and 2 summarize the structures of the *N*-glycans expressed by NSCs before and after differentiation. The most remarkable features were the disappearance of the Lewis X-carrying *N*-glycans, which were ~20% of total *N*-glycans in NSCs, and a concomitant increase in the populations of pauci-mannose-type glycans after cell differentiation.

Selective expression of Lewis X carbohydrates in undifferentiated NSCs was confirmed by Western blotting and immunocytochemical analysis (Fig. 3). As shown in Fig. 3A, two Lewis X-positive bands were clearly detected in NSCs that became almost undetectable after differentiation, however, irrespective of differentiation, neither Lewis A nor sialyl-Lewis X epitopes were detected. In our previous study, the major Lewis X carrier protein with an apparent mass of 90 kDa was identified as a lysosome-associated membrane protein 1 (LAMP-1) (Fig. 3A) (36). The other Lewis X-positive 280-kDa protein was identified as the extracellular matrix protein TNC by MS-based proteomics analyses (supplemental Fig. 2). Furthermore, to determine whether Lewis X epitopes were carried by *N*- or *O*-glycans, we treated the cell lysates with peptide *N*-glycanase F and then analyzed the lysates by Western blotting with an

Lewis X Regulates Notch Signaling in Neural Stem Cells

TABLE 1

The structure and incidence of neutral and desialylated anionic PA-N-glycans derived from NSCs before and after differentiation

Peaks ^b	ODS (GU) ^c	Structures ^d	ratio (mol %) ^e		Peaks ^b	ODS (GU) ^c	Structures ^d	ratio (mol %) ^e	
			Undiffer	Differ				Undiffer	Differ
Neutral glycans									
					N18	11.3		-	1.5
N1	4.8		12.7	8.5	N19	11.6		0.9	-
N2-1°	5.1		6.9	10.5	N20	12.7		2.5	2.0
N2-2°	5.1		9.2	4.5	N21	13.6		1.2	-
N3-1°	6		8.8	5.7	N22	13.9		-	1.6
N3-2°	6		2.2	-	N23	15.2		3.0	-
N4	6.2		2.3	-	N24	15.9		1.3	-
N5-1°	6.2		-	0.5	N25	18		5.1	2.7
N5-2°	6.2		-	0.9	N26	19.3		-	3.1
N6	7		13.0	16.6	N27	21		-	1.0
N7	7.4		2.3	4.0	others			6.1	8.3
N8	7.7		-	1.1	Desialylated anionic glycans (neutral fractions)				
N9-1°	8.6		0.4	-	AN1	7.9		0.5	1.3
N9-2°	8.6		0.3	1.1	AN2	9.4		1.7	-
N9-3°	8.6		0.2	-	AN3-1°	10.3		0.8	0.5
N10-1°	9.1		0.8	-	AN3-2°	10.3		-	0.5
N10-2°	9.1		0.6	-	AN4	10.5		-	1.1
N11	9.5		-	1.9	AN5	10.9		-	1.4
N12-1°	9.5		1.6	-	AN6	11.3		-	1.1
N12-2°	9.5		0.8	-	AN7	12.4		2	-
N13-1°	9.9		0.6	8.6	AN8-1°	14.1		-	0.8
N13-2°	9.9		0.3	-	AN8-2°	14.1		0.9	0.8
N14	10.1		1.7	7.2	AN8-3°	14.1		0.3	-
N15	10.6		1.1	-	others			3.2	-
N16	11		1.3	-	Desialylated anionic glycans (anionic fractions)				
N17-1°	11.3		1.2	-					
N17-2°	11.3		1.2	-				1.2	1.1

^a The ratio (mol %) was calculated from the peak area in Fig. 2 by comparison with the total N-glycan content in NSCs before and after differentiation.

^b Alphanumerical characters (e.g. N1 and DN1) correspond to the individual peaks in Fig. 2.

^c Structures of PA-oligosaccharides are represented using the following symbols: blue circle, glucose (Glc); yellow circle, galactose (Gal); blue square, N-acetylglucosamine (GlcNAc); green circle, mannose (Man); and red triangle, fucose (Fuc).

^d Units of glucose (GU) were calculated from the elution times of the peaks obtained from the ODS column in Fig. 2.

^e Molar percent of individual glycans in a single peak was calculated on the basis of peak intensity on the MALDI-TOF-MS data.

TABLE 2

N-Glycan types expressed by NSCs before and after differentiation

N-Glycans	Ratio	
	Undifferentiation	Differentiation
<i>mol %</i>		
Neutral fraction		
Lewis X-type	15.7	-
Pauci-mannose-type	4.6	19.7
High mannose-type	52.8	47.1
Anionic fraction		
Lewis X-type	4.0	-

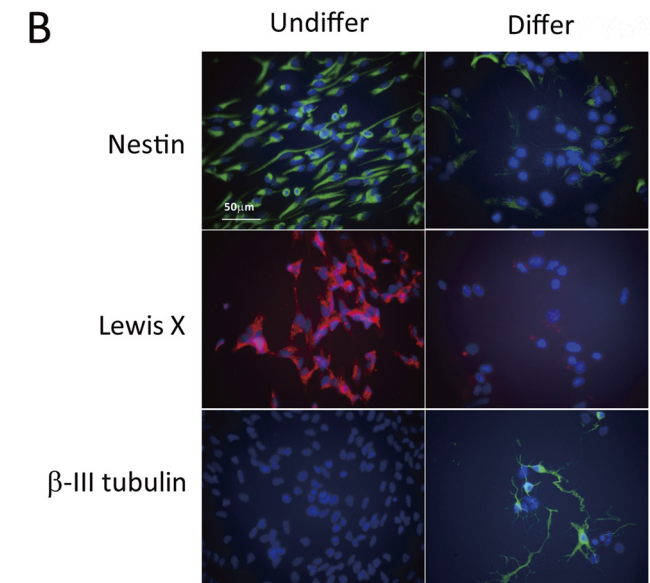
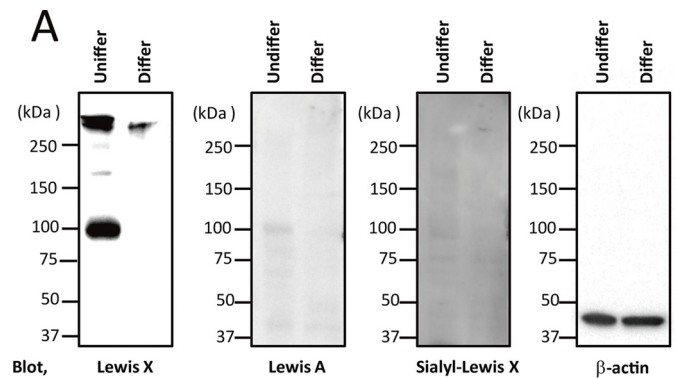


FIGURE 3. Specific expression of Lewis X-carrying glycans in NSCs.

A, lysates prepared from neurospheres and cells differentiated from neurospheres were analyzed by Western blotting with anti-Lewis X, anti-Lewis A, anti-sialyl Lewis X, or anti- β -actin antibodies (Blot). β -Actin was detected as a loading control. **B**, NSCs prepared from neurospheres were treated with PBS containing 3% fetal bovine serum and 0.1% Triton X-100, and then stained with anti-Nestin, anti-Lewis X, and β -III tubulin antibodies as primary antibodies, and Alexa Fluor 488-conjugated anti-rat IgG (green), Alexa Fluor 595-conjugated anti-mouse IgM (red), and Alexa Fluor 488-conjugated anti-mouse IgG antibodies (green) as secondary antibodies. Nuclei were stained with 2 μ g/ml Hoechst 33258 (blue). Undiffer and Differ indicate NSCs before and after differentiation, respectively.

anti-Lewis X antibody (supplemental Fig. 3). After peptide N-glycanase F treatments, the Lewis X-positive bands corresponding to these proteins diminished; the LAMP-1 band was completely abolished, and the TNC band became faintly stained and downward-shifted, which confirmed that Lewis X epitopes are predominantly expressed in the N-glycans of these proteins.

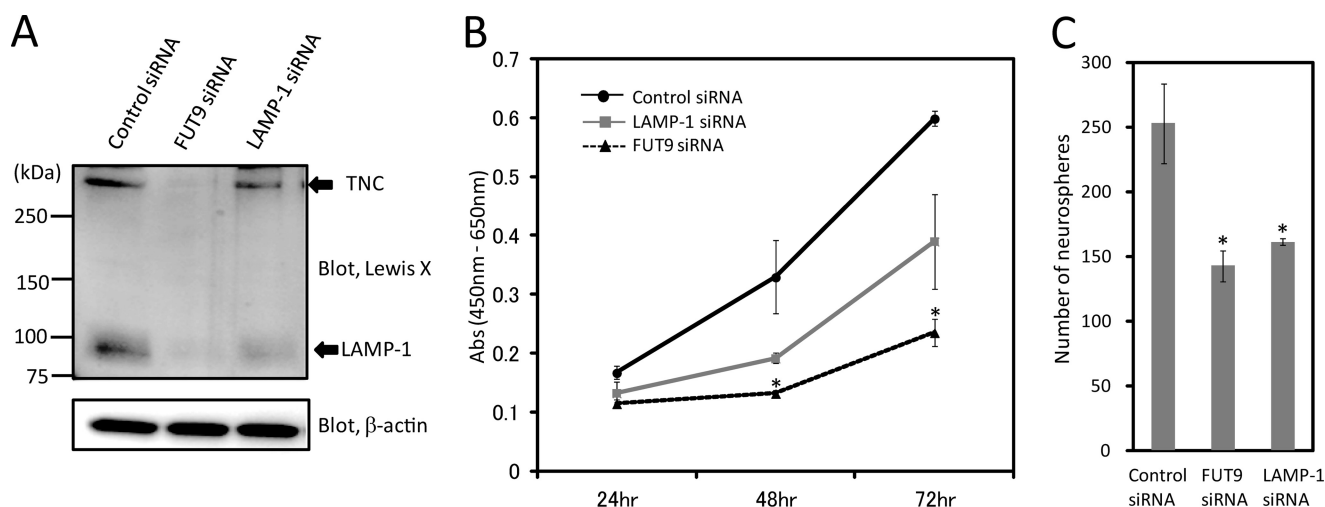


FIGURE 4. Effect of suppression of Lewis X expression on the proliferation of NSCs. A, Western blot of NSCs treated with FUT9, LAMP-1, or scrambled negative control siRNA. Samples were collected after 72 h of siRNA treatment and then subjected to Western blot analysis with anti-Lewis X and anti- β -actin antibodies. β -Actin was detected as a loading control. B, effects of knockdown of FUT9 and LAMP-1 by siRNAs on the proliferation of NSCs. NSCs transfected with FUT9 or negative control siRNAs were cultured as neurospheres for 72 h. Values are means \pm S.D., $n = 4$. Statistical analyses were performed using a two-tailed unpaired Student's test, $*p < 0.01$. C, proliferation rates of neurosphere-forming cells were measured using a WST-8 assay at 72 h after siRNA transfection. Values are means \pm S.D., $n = 4$. Statistical analyses were performed using a two-tailed unpaired Student's test, $*p < 0.01$.

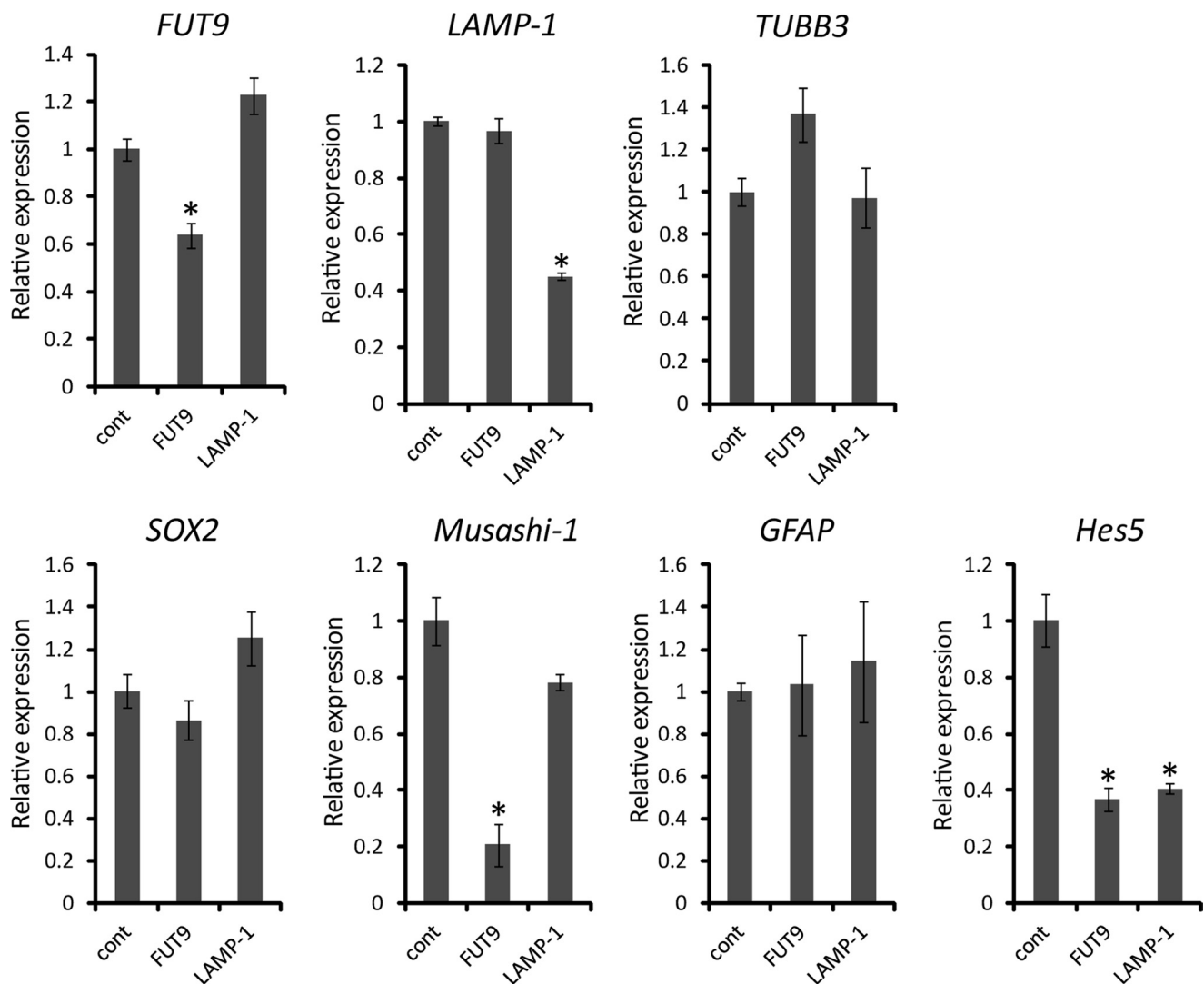


FIGURE 5. Gene expression in NSCs transfected with FUT9 and LAMP-1 siRNAs. Expression levels of NSC-specific (*SOX2* and *Musashi-1*), neuron-specific (*TUBB3*), astrocyte-specific (*GFAP*), and Notch signaling-related (*Hes5*) genes were analyzed by quantitative RT-PCR. Samples were collected after 48 h of siRNA treatment. Values are means \pm S.D., $n = 3$. Statistical analyses were performed using a two-tailed unpaired Student's test; $*p < 0.01$; cont, control.

Lewis X Regulates Notch Signaling in Neural Stem Cells

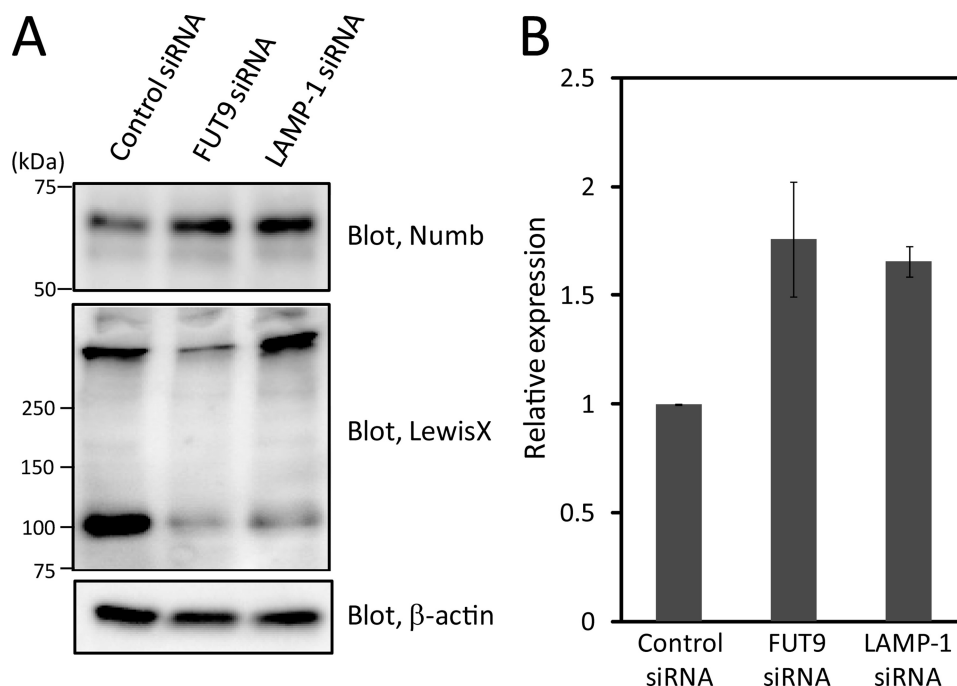


FIGURE 6. **Modulation of Notch-1 signaling by the expression of Lewis X glycotopes.** *A*, Western blot of NSCs treated with FUT9, LAMP-1, or negative control siRNA using anti-Numb-1, anti-Lewis X, and β -actin antibodies. β -Actin was detected as a loading control. *B*, expression level of Numb-1 measured by densitometric analysis using a scanning densitometer. Data are expressed relative to an internal loading control (β -actin) and as means \pm S.E., $n = 3$.

Effects of FUT9 Knockdown by siRNA on the Proliferation of NSCs—In our previous study (36), the mRNA expression level of fucosyltransferase 9 (FUT9) was found to be down-regulated in cells that differentiated from NSCs, compared with the expression levels of other α 1,3-fucosyltransferases. Transfection with siRNA of FUT9 or LAMP-1 with siRNA caused a reduction in Lewis X expression (Fig. 4A). This indicated that FUT9 is primarily responsible for the fucosylation process that gives rise to the Lewis X glycotopes that are displayed specifically on LAMP-1 in NSCs. Intriguingly, the suppression of FUT9 or LAMP-1 expression by siRNA resulted in a reduction of the number of NSCs (Fig. 4B) and a decrease in their ability to form neurospheres (Fig. 4C), which was evaluated by the WST-8 assay (32, 33); however, there was no significant difference in the number of NSCs that were positive for TUNEL, which is an indicator of cell death accompanied by DNA fragmentation (supplemental Fig. 4A). Furthermore, in the FUT9-suppressed cells, there was no activation of caspase-3, which is a critical executioner of apoptosis or programmed cell death signaling (supplemental Fig. 4B). Thus, these knockdown analyses revealed that the Lewis X glycotopes expressed on LAMP-1 promotes the proliferation of NSCs without affecting the cell death pathways.

Modulation of the Notch Signaling Pathway by Lewis X Glycotopes—To analyze the molecular mechanism that couples the suppression of Lewis X expression to the down-regulation of NSC proliferation, we investigated the gene expression of undifferentiation (*Sox2* and *Musashi-1*) and differentiation (*GFAP* and *TUBB3*) markers. In NSCs transfected with FUT9 siRNAs, a significant decrease in *Musashi-1* levels and slight increases in *GFAP* and *TUBB3* levels were detected (Fig. 5). It has been reported that the *Musashi-1* protein positively regulates Notch signaling through the reduction of the translation

of Numb, which is an inhibitor of the Notch signaling pathway (13, 14). Our data also demonstrated that Numb expression was enhanced in the FUT9 knockdown cell (Fig. 6), accompanied with a reduced expression of *Hes5* (Fig. 5), which is one of the downstream molecules in the Notch signaling pathway.

DISCUSSION

In this study, we demonstrated that the *N*-glycosylation profiles of NSCs changed dramatically during their development. In particular, the Lewis X-carrying *N*-glycans were specifically expressed on NSCs, whereas pauci-mannose-type glycans were predominantly expressed on differentiated cells (Tables 1 and 2). In our analytical procedure, *N*-glycans were derived from the cell membranes and the intracellular compartments. In general, the pauci-mannose-type *N*-glycans do not arise from the *N*-glycans processing in the secretory pathway but appear during the *N*-glycans degradation process in cells (37). The altered expression patterns of the pauci-mannose-type oligosaccharides before and after differentiation suggest the possible switching of different degradation pathways or lysosomal maturation during NCS differentiation.

Lewis X is a well known stage-specific marker (termed SSEA-1) of undifferentiated cells, including human embryonic NSCs and mouse embryonic, postnatal, and adult NSCs (10, 11, 38). Our knockdown experiment demonstrated that FUT9 is responsible for the formation of Lewis X in NSCs (Fig. 4A). Impaired expression of *FUT9* mRNA and the subsequent depletion of Lewis X were also reported in the embryonic brain of the rat *small eye* strain, which has a mutation in *Pax6* (39). *Pax6* is expressed in NSCs as a key regulator of self-renewal and neurogenesis (40). Overall, these data suggest that the expression of the Lewis X glycotopes in undifferentiated NSCs is controlled by *Pax6* via up-regulation of the FUT9 levels.

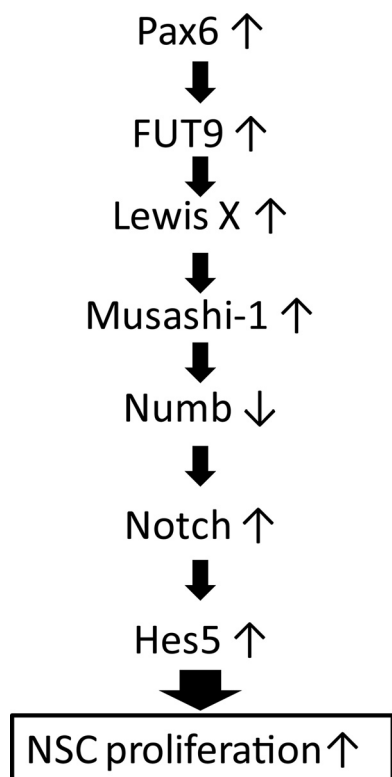


FIGURE 7. Schematic representation for the up-regulating mechanism of NSC proliferation by modulating Notch signaling with Lewis X-containing glycans in NSCs.

It has been reported that NSCs treated with an organic solvent to wash out cell surface glycolipids have strong immunoreactivity with anti-Lewis X antibody (41), indicating that this glycotope is carried mainly by glycoproteins and/or proteoglycans rather than glycolipids. To date, phosphacan, CD24, integrin, L1-CAM, Thy-1, LAMP-1, and TNC have been identified as Lewis X-carrying proteins (36, 38, 42–45). Here, we demonstrated that LAMP-1 and TNC are major Lewis X carriers in NSCs (Fig. 3A). In particular, this study highlights that LAMP-1 displays Lewis X glycotope(s) specifically on its *N*-glycans, exclusively in undifferentiated NSCs. LAMP-1 is a well known lysosomal marker, but this protein has also been reported to be expressed on tumor cell surfaces, where it mediates cell-cell communication through interactions with sugar-binding proteins such as galectin-3 and E-selectin (46, 47). Thus, Lewis X-carrying LAMP-1 on NSCs might function through interactions with putative lectin(s) that recognize this glycotope and express the signals leading to cell proliferation.

Although Lewis X has been implicated to be involved in cellular aggregation and migration in NSCs (38, 48, 49), to the best of our knowledge there have been no previous reports that Lewis X is engaged in signal transduction during NSC fate determination. In this study, we elucidated a signaling pathway in which Lewis X expression has been shown to be associated with proliferation of NSCs. FUT9-siRNA-treated NSCs led to reduced mRNA expression levels of Musashi-1 (Fig. 5), which is an RNA-binding protein that serves as another NSC marker. Musashi-1 protein binds to *Numb* mRNA and inhibits its translation (13, 14). *Numb* protein binds to the intracellular domain

of Notch protein, thereby precluding the activation of the Notch pathway, presumably by guiding Notch protein from the cell surface to the endosome-mediated degradation pathway (50). Indeed, we demonstrated that abrogation of *FUT9* expression is coupled with an increased *Numb* level (Fig. 6), eventually resulting in the suppression of Notch signaling, as exemplified by reduced *Hes5* expression (Fig. 5). The activation of the Notch pathway positively regulates the self-renewal and proliferation of NSCs (16, 51, 52). Our findings provide insights into the functional role of the Lewis X groups displayed on *N*-glycans that operate as active modulators of Notch signaling for the maintenance of NSC stemness during brain development (Fig. 7).

REFERENCES

- Gage, F. H. (2000) Mammalian neural stem cells. *Science* **287**, 1433–1438
- McKay, R. (1997) Stem cells in the central nervous system. *Science* **276**, 66–71
- Temple, S., and Alvarez-Buylla, A. (1999) Stem cells in the adult mammalian central nervous system. *Curr. Opin. Neurobiol.* **9**, 135–141
- Temple, S. (1989) Division and differentiation of isolated CNS blast cells in microculture. *Nature* **340**, 471–473
- Doetsch, F., Caillé, I., Lim, D. A., García-Verdugo, J. M., and Alvarez-Buylla, A. (1999) Subventricular zone astrocytes are neural stem cells in the adult mammalian brain. *Cell* **97**, 703–716
- Seri, B., García-Verdugo, J. M., McEwen, B. S., and Alvarez-Buylla, A. (2001) Astrocytes give rise to new neurons in the adult mammalian hippocampus. *J. Neurosci.* **21**, 7153–7160
- Lendahl, U., Zimmerman, L. B., and McKay, R. D. (1990) CNS stem cells express a new class of intermediate filament protein. *Cell* **60**, 585–595
- Uchida, N., Buck, D. W., He, D., Reitsma, M. J., Masek, M., Phan, T. V., Tsukamoto, A. S., Gage, F. H., and Weissman, I. L. (2000) Direct isolation of human central nervous system stem cells. *Proc. Natl. Acad. Sci. U.S.A.* **97**, 14720–14725
- Zappono, M. V., Galli, R., Catena, R., Meani, N., De Biasi, S., Mattei, E., Tiveron, C., Vescovi, A. L., Lovell-Badge, R., Ottolenghi, S., and Nicolini, S. K. (2000) Sox2 regulatory sequences direct expression of a β -geo transgene to telencephalic neural stem cells and precursors of the mouse embryo, revealing regionalization of gene expression in CNS stem cells. *Development* **127**, 2367–2382
- Klassen, H., Schwartz, M. R., Bailey, A. H., and Young, M. J. (2001) Surface markers expressed by multipotent human and mouse neural progenitor cells include tetraspanins and non-protein epitopes. *Neurosci. Lett.* **312**, 180–182
- Capela, A., and Temple, S. (2002) LeX/ssea-1 is expressed by adult mouse CNS stem cells, identifying them as nonpendymal. *Neuron* **35**, 865–875
- Sakakibara, S., Nakamura, Y., Yoshida, T., Shibata, S., Koike, M., Takano, H., Ueda, S., Uchiyama, Y., Noda, T., and Okano, H. (2002) RNA-binding protein Musashi family. Roles for CNS stem cells and a subpopulation of ependymal cells revealed by targeted disruption and antisense ablation. *Proc. Natl. Acad. Sci. U.S.A.* **99**, 15194–15199
- Imai, T., Tokunaga, A., Yoshida, T., Hashimoto, M., Mikoshiba, K., Weinmaster, G., Nakafuku, M., and Okano, H. (2001) The neural RNA-binding protein Musashi1 translationally regulates mammalian *numb* gene expression by interacting with its mRNA. *Mol. Cell. Biol.* **21**, 3888–3900
- Okano, H., Kawahara, H., Toriya, M., Nakao, K., Shibata, S., and Imai, T. (2005) Function of RNA-binding protein Musashi-1 in stem cells. *Exp. Cell Res.* **306**, 349–356
- Nakashima, K., Wiese, S., Yanagisawa, M., Arakawa, H., Kimura, N., Hitsuji, T., Yoshida, K., Kishimoto, T., Sendtner, M., and Taga, T. (1999) Developmental requirement of gp130 signaling in neuronal survival and astrocyte differentiation. *J. Neurosci.* **19**, 5429–5434
- Hitoshi, S., Alexson, T., Tropepe, V., Donoviel, D., Elia, A. J., Nye, J. S., Conlon, R. A., Mak, T. W., Bernstein, A., and van der Kooy, D. (2002) Notch pathway molecules are essential for the maintenance, but not the generation, of mammalian neural stem cells. *Genes Dev.* **16**, 846–858

17. Campos, L. S., Leone, D. P., Relvas, J. B., Brakebusch, C., Fässler, R., Suter, U., and French-Constant, C. (2004) $\beta 1$ integrins activate a MAPK signaling pathway in neural stem cells that contributes to their maintenance. *Development* **131**, 3433–3444
18. Backman, M., Machon, O., Mygland, L., van den Bout, C. J., Zhong, W., Taketo, M. M., and Krauss, S. (2005) Effects of canonical Wnt signaling on dorso-ventral specification of the mouse telencephalon. *Dev. Biol.* **279**, 155–168
19. Yanagisawa, M., Nakamura, K., and Taga, T. (2005) Glycosphingolipid synthesis inhibitor represses cytokine-induced activation of the Ras-MAPK pathway in embryonic neural precursor cells. *J. Biochem.* **138**, 285–291
20. Bithell, A., and Williams, B. P. (2005) Neural stem cells and cell replacement therapy. Making the right cells. *Clin. Sci.* **108**, 13–22
21. de Filippis, L. (2011) Neural stem cell-mediated therapy for rare brain diseases. Perspectives in the near future for LSDs and MNDs. *Histol. Histopathol.* **26**, 1093–1109
22. Yagi, H., Yanagisawa, M., Suzuki, Y., Nakatani, Y., Ariga, T., Kato, K., and Yu, R. K. (2010) HNK-1 epitope-carrying tenascin-C spliced variant regulates the proliferation of mouse embryonic neural stem cells. *J. Biol. Chem.* **285**, 37293–37301
23. Yanagisawa, M., Kojima, H., Kawakami, Y., Iriko, H., Nakamura, T., Nakamura, K., Uchida, A., Murata, Y., and Tamai, Y. (1999) A monoclonal antibody against a glycolipid SEGLx from *Spirometra erinaceieuropaei* plerocercoid. *Mol. Biochem. Parasitol.* **102**, 225–235
24. Nakatani, Y., Yanagisawa, M., Suzuki, Y., and Yu, R. K. (2010) Characterization of GD3 ganglioside as a novel biomarker of mouse neural stem cells. *Glycobiology* **20**, 78–86
25. Nakagawa, H., Kawamura, Y., Kato, K., Shimada, I., Arata, Y., and Takahashi, N. (1995) Identification of neutral and sialyl *N*-linked oligosaccharide structures from human serum glycoproteins using three kinds of high performance liquid chromatography. *Anal. Biochem.* **226**, 130–138
26. Takahashi, N., and Kato, K. (2003) GALAXY (Glycoanalysis by the Three Axes of MS and Chromatography): a Web Application That Assists Structural Analyses of *N*-Glycans. *Trends Glycosci. Glycotech.* **15**, 235–251
27. Yagi, H., Takahashi, N., Yamaguchi, Y., Kimura, N., Uchimura, K., Kannagi, R., and Kato, K. (2005) Development of structural analysis of sulfated *N*-glycans by multidimensional high performance liquid chromatography mapping methods. *Glycobiology* **15**, 1051–1060
28. Yagi, H., Nakagawa, M., Takahashi, N., Kondo, S., Matsubara, M., and Kato, K. (2008) Neural complex-specific expression of xylosyl *N*-glycan in *Ciona intestinalis*. *Glycobiology* **18**, 145–151
29. Tanabe, K., and Ikenaka, K. (2006) In-column removal of hydrazine and *N*-acetylation of oligosaccharides released by hydrazinolysis. *Anal. Biochem.* **348**, 324–326
30. Yagi, H., Yamamoto, M., Yu, S. Y., Takahashi, N., Khoo, K. H., Lee, Y. C., and Kato, K. (2010) *N*-Glycosylation profiling of turtle egg yolk. Expression of galabiose structure. *Carbohydr. Res.* **345**, 442–448
31. Yagi, H., Yasukawa, N., Yu, S. Y., Guo, C. T., Takahashi, N., Takahashi, T., Bukawa, W., Suzuki, T., Khoo, K. H., Suzuki, Y., and Kato, K. (2008) The expression of sialylated high antennary *N*-glycans in edible bird's nest. *Carbohydr. Res.* **343**, 1373–1377
32. Kanemura, Y., Mori, H., Kobayashi, S., Islam, O., Kodama, E., Yamamoto, A., Nakanishi, Y., Arita, N., Yamasaki, M., Okano, H., Hara, M., and Miyake, J. (2002) Evaluation of *in vitro* proliferative activity of human fetal neural stem/progenitor cells using indirect measurements of viable cells based on cellular metabolic activity. *J. Neurosci. Res.* **69**, 869–879
33. Yanagisawa, M., and Yu, R. K. (2009) *O*-Linked β -*N*-acetylglucosaminylation in mouse embryonic neural precursor cells. *J. Neurosci. Res.* **87**, 3535–3545
34. Suzuki, Y., Yanagisawa, M., Yagi, H., Nakatani, Y., and Yu, R. K. (2010) Involvement of $\beta 1$ -integrin up-regulation in basic fibroblast growth factor- and epidermal growth factor-induced proliferation of mouse neuroepithelial cells. *J. Biol. Chem.* **285**, 18443–18451
35. Reynolds, B. A., and Weiss, S. (1992) Generation of neurons and astrocytes from isolated cells of the adult mammalian central nervous system. *Science* **255**, 1707–1710
36. Yagi, H., Yanagisawa, M., Kato, K., and Yu, R. K. (2010) Lysosome-associated membrane protein 1 is a major SSEA-1-carrier protein in mouse neural stem cells. *Glycobiology* **20**, 976–981
37. Moriguchi, K., Takemoto, T., Aoki, T., Nakakita, S., Natsuka, S., and Hase, S. (2007) Free oligosaccharides with Lewis x structure expressed in the segmentation period of zebrafish embryo. *J. Biochem.* **142**, 213–227
38. Yanagisawa, M., Taga, T., Nakamura, K., Ariga, T., and Yu, R. K. (2005) Characterization of glycoconjugate antigens in mouse embryonic neural precursor cells. *J. Neurochem.* **95**, 1311–1320
39. Shimoda, Y., Tajima, Y., Osanai, T., Katsume, A., Kohara, M., Kudo, T., Narimatsu, H., Takashima, N., Ishii, Y., Nakamura, S., Osumi, N., and Sanai, Y. (2002) Pax6 controls the expression of Lewis x epitope in the embryonic forebrain by regulating $\alpha 1,3$ -fucosyltransferase IX expression. *J. Biol. Chem.* **277**, 2033–2039
40. Sansom, S. N., Griffiths, D. S., Faedo, A., Kleinjan, D. J., Ruan, Y., Smith, J., van Heyningen, V., Rubenstein, J. L., and Livesey, F. J. (2009) The level of the transcription factor Pax6 is essential for controlling the balance between neural stem cell self-renewal and neurogenesis. *PLoS Genet.* **5**, e1000511
41. Yanagisawa, M., Yoshimura, S., and Yu, R. K. (2011) Expression of GD2 and GD3 gangliosides in human embryonic neural stem cells. *ASN Neuro.* **3**, pii e00054
42. Streit, A., Faissner, A., Gehrig, B., and Schachner, M. (1990) Isolation and biochemical characterization of a neural proteoglycan expressing the L5 carbohydrate epitope. *J. Neurochem.* **55**, 1494–1506
43. Garwood, J., Schnädelbach, O., Clement, A., Schütte, K., Bach, A., and Faissner, A. (1999) DSD-1-proteoglycan is the mouse homolog of phosphacan and displays opposing effects on neurite outgrowth dependent on neuronal lineage. *J. Neurosci.* **19**, 3888–3899
44. Lieberoth, A., Splittstoesser, F., Katagihallimath, N., Jakovcevski, I., Loers, G., Ranscht, B., Karageorgos, D., Schachner, M., and Kleene, R. (2009) Lewis^x and $\alpha 2,3$ -sialyl glycans and their receptors TAG-1, Contactin, and L1 mediate CD24-dependent neurite outgrowth. *J. Neurosci.* **29**, 6677–6690
45. Hennen, E., Czopka, T., and Faissner, A. (2011) Structurally distinct Lewis X glycans distinguish subpopulations of neural stem/progenitor cells. *J. Biol. Chem.* **286**, 16321–16331
46. Sarafian, V., Jadot, M., Foidart, J. M., Letesson, J. J., Van den Brùle, F., Castronovo, V., Wattiaux, R., and Coninck, S. W. (1998) Expression of Lamp-1 and Lamp-2 and their interactions with galectin-3 in human tumor cells. *Int. J. Cancer* **75**, 105–111
47. Tomlinson, J., Wang, J. L., Barsky, S. H., Lee, M. C., Bischoff, J., and Nguyen, M. (2000) Human colon cancer cells express multiple glycoprotein ligands for E-selectin. *Int. J. Oncol.* **16**, 347–353
48. Eggens, I., Fenderson, B., Toyokuni, T., Dean, B., Stroud, M., and Hakomori, S. (1989) Specific interaction between Lex and Lex determinants. A possible basis for cell recognition in preimplantation embryos and in embryonal carcinoma cells. *J. Biol. Chem.* **264**, 9476–9484
49. Streit, A., Nolte, C., Rásony, T., and Schachner, M. (1993) Interaction of astrochondrin with extracellular matrix components and its involvement in astrocyte process formation and cerebellar granule cell migration. *J. Cell Biol.* **120**, 799–814
50. Berdnik, D., Török, T., González-Gaitán, M., and Knoblich, J. A. (2002) The endocytic protein α -Adaptin is required for numb-mediated asymmetric cell division in *Drosophila*. *Dev. Cell* **3**, 221–231
51. Chen, J., Zacharek, A., Li, A., Cui, X., Roberts, C., Lu, M., and Chopp, M. (2008) Atorvastatin promotes presenilin-1 expression and Notch1 activity and increases neural progenitor cell proliferation after stroke. *Stroke* **39**, 220–226
52. Zhou, Z. D., Kumari, U., Xiao, Z. C., and Tan, E. K. (2010) Notch as a molecular switch in neural stem cells. *IUBMB Life* **62**, 618–623